ACS Photonics

Article

pubs.acs.org/journal/apchd5

Exploring Light–Matter Interaction Phenomena under Ultrastrong Coupling Regime

Salvatore Gambino,[†,§] Marco Mazzeo,[*,‡,§] Armando Genco,[§] Omar Di Stefano,[∥] Salvatore Savasta,[∥] Salvatore Patanè,[∥] Dario Ballarini,[§] Federica Mangione,[§] Giovanni Lerario,[†,‡] Daniele Sanvitto,[§] and Giuseppe Gigli[†,‡,§]

[†]CBN, Istituto Italiano di Tecnologia, Via Barsanti 1, 73010 Lecce, Italy

[‡]Dipartimento di Matematica e Fisica "Ennio De Giorgi", Università del Salento, Via per Arnesano, 73100 Lecce, Italy

[§]NNL, Istituto Nanoscienze–CNR, Via [er Arnesano, 73100 Lecce, Italy

[∥]Dipartimento di Fisica e di Scienze e della Terra, Università di Messina, Viale F. Stagno d'Alcontres 31, 98166 Messina, Italy

Supporting Information

ABSTRACT: Exciton-polaritons are bosonic quasiparticles that arise from the normal mode splitting of photons in a microcavity and excitons in a semiconductor material. One of the most intriguing extensions of such a light–matter interaction is the so-called ultrastrong coupling regime. It is achieved when the Rabi frequency (Ω_R, the energy exchange rate between the emitter and the resonant photonic mode) reaches a considerable fraction of the emitter transition frequency, ω_0. Here, we report a Rabi energy splitting ($2\hbar\Omega_R$) of 1.12 eV and record values of the coupling ratio ($2\Omega_R/\omega_0$) up to 0.6-fold the material band gap in organic semiconductor microcavities and up to 0.5-fold in monolithic heterostructure organic light-emitting diodes working at room temperature. Furthermore, we show that with such a large coupling strength it is possible to undress the exciton homogeneous linewidth from its inhomogeneous broadening, which allows for an unprecedented narrow emission line (below the cavity finesse) for such organic LEDs. The latter can be exploited for the realization of novel monochromatic sources and near-IR organic emitting devices.

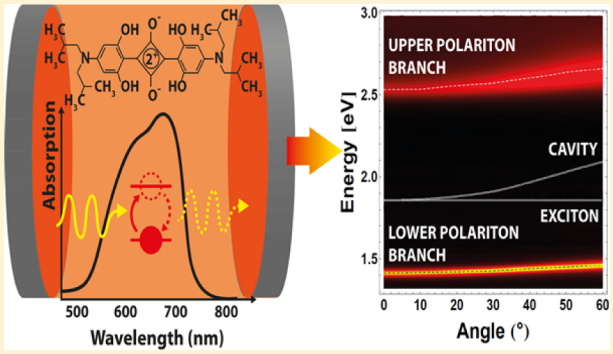

KEYWORDS: *polaritons, light–matter interactions, Rabi splitting, ultrastrong coupling, organic microcavities, organic light-emitting diodes*

Light–matter interaction in the strong coupling (SC) regime is a reversible process in which a dipole, optically coupled with a resonator, absorbs and reemits a photon before losses take place. The rate at which this exchange occurs is called vacuum Rabi frequency (Ω_R). Under such a regime new hybrid light–matter states, called polaritons, are formed, which are the result of the splitting of the two normal modes of the system. These bosonic quasi-particles, a mixture of excitons and photons, are particularly interesting for their very low mass, easy optical control, and the possibility to show Bose–Einstein condensation[1,2] at high temperatures.[3] Polaritons have also shown very intriguing superfluid related phenomena[4,5] and quantized hydrodynamics effects[6,7] and could be exploited for the realization of all-optical circuits[8] and photonic quantum devices.[9] Recently a new regime of cavity quantum electrodynamics (cavity-QED), where the vacuum Rabi frequency becomes an appreciable fraction of the unperturbed frequency of the system, has been experimentally reached.[10] In this so-called ultrastrong coupling (USC)[11,12] regime the routinely invoked rotating wave approximation (RWA) is no longer applicable, and the antiresonant terms significantly change the standard cavity-QED scenarios.[13−18]

A key parameter that gives an indication of the effective coupling strength is the normalized coupling factor $g = 2\hbar\Omega_R/\hbar\omega_0$, where $2\hbar\Omega_R$ is the Rabi energy splitting, i.e., the minimum energy difference between the two new hybrid states, and $\hbar\omega_0$ is the material transition energy. When the Rabi energy is a significant fraction of the material transition energy, i.e., g is larger than 20%, the USC features start to manifest.[15] To this purpose it is needed to minimize ω_0 or maximize Ω_R. In the first case, it is possible to use small energy band gap materials, such as in the THz spectral region.[10,19,20] Recently remarkable couplings have been obtained but at very low working temperatures,[10,20] which is a concern for the development of cost-effective photonic devices. Another way to increase the coupling, given that Ω_R is proportional to $(fN/V)^{1/2}$, is to act on the dipole oscillator strength f, the number of dipoles coupled to the cavity N, or the photonic modal volume V.

Received: July 22, 2014
Published: October 3, 2014

   dx.doi.org/10.1021/ph500266d | *ACS Photonics* 2014, 1, 1042–1048

Organic semiconductors are the ideal candidates for this purpose, because, thanks to their large oscillator strengths, they can favor very strong light−matter couplings at room temperature. Since the pioneering work of Lidzey et al.,[21] organic polariton microcavities have been the subject of an intense investigation. Lately[22] a Rabi splitting of 700 meV and a normalized coupling factor g of about 32% have been shown using a spin-coated film of spiropyran molecules in a PMMA matrix. More recently, a remarkable Rabi splitting (∼1 eV) in a microcavity working in the UV spectral region with a similar coupling factor has also been reported.[23]

In the present work we used a squaraine-filled microcavity to realize a Rabi splitting of 1120 meV, which corresponds to a normalized coupling strength value of 60% under optical excitation and nearly 50% under electrical injection, which is almost twice the value that we have recently reported.[24] This has been achieved thanks to a careful optimization of the multilayer microcavity OLED, based on p−i−n technology, that has allowed us to reach the best trade-off between the optical coupling parameters and the electrical constraints.

Moreover, thanks to the coherent coupling of all the inhomogeneously broadened dipoles inside the cavity, we demonstrate polariton electroluminescent emission with a linewidth 12-fold narrower than the bare material photoluminescence and even twice as narrow than the optical mode. We believe that these results open the way for the realization of new electroluminscent devices such as very narrow and angle-independent monochromatic organic light sources.[25,3]

RESULTS AND DISCUSSION

Our microcavity is realized using a high-vacuum thermally evaporable dye that belongs to the family of squaraine derivatives. This class of material offers the unique possibility to be designed with tunable optical properties in the vis−IR range, which allows their use in electronic and photonic devices.[26−30] In order to satisfy the initial requirements, such as a material characterized by a large oscillator strength, we choose, within the class of the squaraine family, one that was thermally stable and having a large absorbance (dashed line in Figure 1a).[31] The chemical structure of the squaraine dye is shown in Figure S1, together with a schematic representation of the microcavity. We focus first on the optical characterization of the microcavity, to demonstrate that our system is fully working in the USC regime. All the results that will be discussed thereafter have been carried out at room temperature. The transmission spectra at zero exciton-cavity detuning are reported in Figure 1a for the full and the bare cavity (black and red solid lines, respectively). As can be seen, using a neat film of squaraine, fully filling the entire cavity volume (140 nm), we reached a Rabi energy splitting of 1.12 eV. This energy difference normalized to the exciton energy gave a coupling factor of about 60%, experimentally proving that we are well into the USC regime, where deviations from the RWA model appear as the coupling energy approaches that of the material transition energy.[22,23] This is the first time that such a high level of coupling is reached in an organic semiconductor and at visible wavelength. In Figure 1b, the angle-dependent transmission measurements, under TE polarized light, are shown, for the full cavity (contour plot) together with the bare cavity dispersion (circular dots). Both upper and lower polariton branches display an almost dispersionless behavior all over the angular range investigated. The transmission spectra at different angles of incidence have also been theoretically calculated by

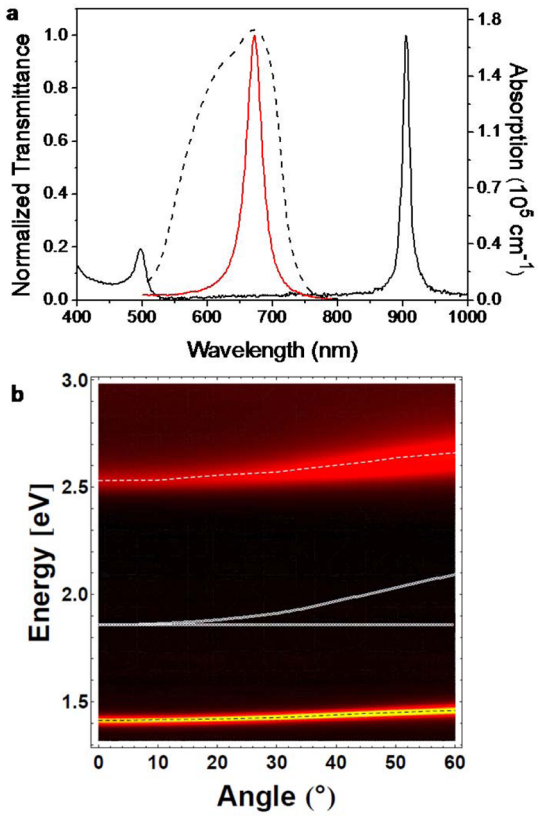

Figure 1. USC microcavity optical characterization. (a) Absorption spectrum of 140 nm squarine neat film (dashed line); normalized transmission spectra (black solid line) of the Ag/140 nm squaraine/Ag microcavity at normal angle in USC regime with a coupling of 60% and of the bare cavity (red solid line). (b) Contour plots taken at room temperature and for TE polarization of the angle-resolved transmission spectra for the microcavity. The dashed lines trace the lower and upper polariton branches calculated using the transfer matrix method. Bare cavity dispersion and exciton energy (circular dots).

employing the transfer matrix method (TMM),[32] which automatically takes into account the counter-rotating terms in the interaction. The complex refractive index of the film used in the calculations has been obtained from the experimental absorbance by means of a Kramers−Kronig procedure.[33] Calculations have been performed without any adjustable parameters, yet it is noticeable that they extremely well describe the experimental data.

A crucial point to address here is the demonstration that the squaraine dye really drives the cavity into the strong coupling regime with coherent energy exchange between photon and exciton. Reports on J-aggregates with a peak extinction coefficient of about an order of magnitude larger compared to the squaraine showed a much smaller splitting.[29] Actually, Houdrè et al.[34] have reported that the vacuum Rabi splitting depends on the energy-integrated absorption rather than on just the absorption peak. Specifically they showed that the peak separation of the splitting is independent of the homogeneous or inhomogeneous nature of the electronic oscillator strength, which depends on the energy integrated absorption according to the Smakula formula:[35]

$$Nf = 8.21 \times 10^{15}\ \mathrm{cm}^{-3} \frac{n}{(n^2+2)^2} \int \alpha(E)\, \mathrm{d}E \qquad (1)$$

dx.doi.org/10.1021/ph500266d | ACS Photonics 2014, 1, 1042−1048

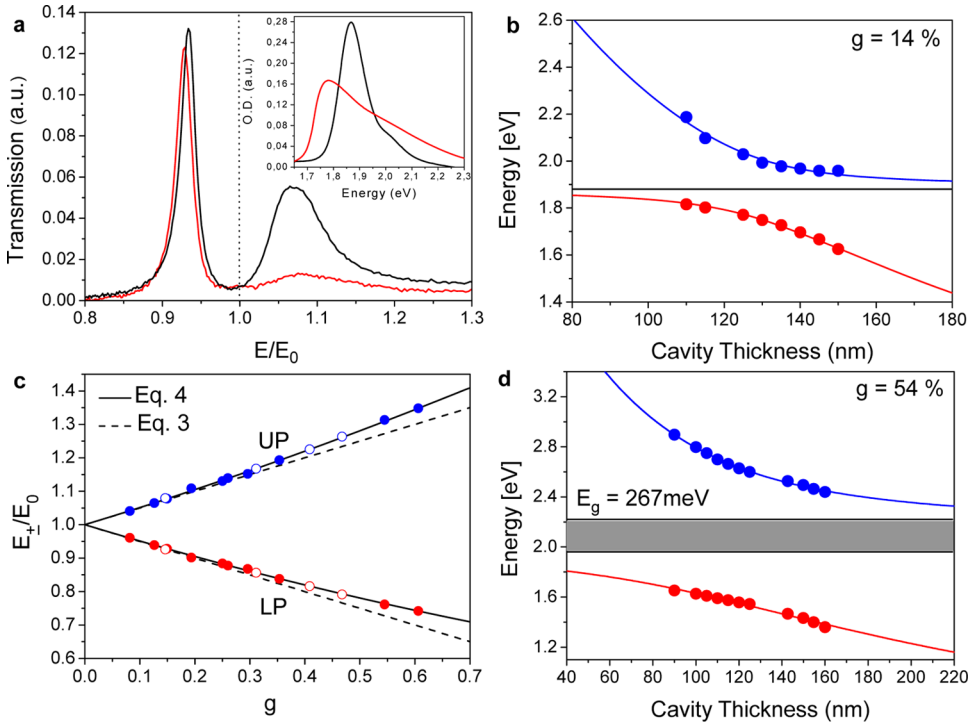

Figure 2. Characteristic features of the strong and ultrastrong coupling regime. (a) Transmission polariton spectra normalized to the exciton energy, E_0, of a heterostructure microcavity (red line) and a diluted cavity having the same integrated optical density but different spectral broadenings. Inset: Absorption spectra of the squaraine layer used in the two cavities. Black line is the absorption spectrum of a diluted squaraine film, while the red line represents that of a neat film of squaraine embedded into the heterostructure microcavity. The same absorption integral results in the same energy splitting and coupling (g = 14%). (b) Polariton energy maxima for both upper polariton (UP) and lower polariton (LP) branches of a cavity at g = 14%. Experimental data (circular dots) have been plotted as a function of the cavity thickness (detuning). (c) Polariton maximum energies for both UP and LP branches normalized to the exciton energy. Filled dots are the experimental data for the microcavities, while the open dots are the ones for the heterostructure microcavity OLEDs. In both cases experimental data have been plotted at zero exciton-cavity detuning. Dashed lines represent the polariton eigenvalues of the approximated Hamiltonian, i.e., neglecting the antiresonant terms, while the solid lines represent the polariton eigenvalues of the full Hamiltonian. (d) Polariton energy maxima for both UP and LP branches of a cavity at g = 54%. Experimental data (circular dots) have been plotted as a function of the cavity thickness (detuning). The continuous lines are the roots of eq 2. The shaded region indicates the polariton gap.

Moreover it has been shown theoretically[34] that for large enough vacuum Rabi splitting the linewidth of the polariton peaks is homogeneously broadened. Hence the picture of coherent light−matter coupling is not significantly affected by inhomogeneous broadening, at least for a large splitting. The homogeneously broadened polariton peaks in the transmission spectrum displayed in Figure 1a provide a clear indication of coherent coupling even in the presence of a strong inhomogeneous broadening.

In order to check if the dependence of the Rabi splitting in squaraine-based microcavities on the absorption is in agreement with the theoretical analysis of ref 34, a series of samples have been fabricated with a different number of absorbing dipoles (N) coupled with the electromagnetic field (see SI for further information). Figure 2a (inset) shows the absorption spectra of a microcavity that has been realized by diluting 20% in volume of squaraine into an *N*,*N*′-di[(1-naphthyl)-*N*,*N*′-diphenyl]-1,1′-biphenyl)-4,4′-diamine (NPB) matrix (black line), while the other by placing a 5 nm neat squaraine film in the middle of two buffer layers (red line). In the case of the diluted film the squaraine molecules are far from each other and the absorption spectrum is similar to the diluted liquid solution (see Figure S2), while for the neat film, the stronger intermolecular interaction results in a larger exciton energy distribution. The two samples have different inhomogeneously broadened absorption spectra but the same total oscillator strength; that is, the absorption intensity and spectral shape are different, but the integrated area is the same. In Figure 2a we plotted the transmission spectra as a function of the normalized (to the exciton) energy. Both cavities are tuned at cavity−exciton energy resonance. It can be seen that both lower polariton (LP) and upper polariton (UP) peaks match very well, leading to the same Rabi splitting (260 meV) and coupling (g = 14%).[36] This is an experimental proof that the inhomogeneous broadening of the exciton has no effect on the peak separation of the splitting, thus confirming the SC regime and the coherent coupling of all the oscillators into the new polariton eigenmodes of the systems (the upper and lower branches). This is consistent with previously reported results for systems characterized by inhomogeneous broad exciton oscillators.[34,37] This could be explained in a simple way assuming that, by inserting into an optical resonator a "disordered system" characterized by a large distribution of optical transition states (i.e., broad absorption spectrum), the light−matter interaction is enhanced by the cooperative behavior of this large number of optical transitions at different energies. When this collective resonance is coupled to the cavity mode, the system enters the strong coupling regime, and it can be seen as a single oscillator whose strength is given by the whole oscillations of the dipoles coherently coupled. This is analogous to the case of a multiquantum well system embedded between two metal mirrors.[38,39]

dx.doi.org/10.1021/ph500266d | ACS Photonics 2014, 1, 1042−1048

Generally speaking, the observation of two peaks in reflection or transmission spectrum is a necessary but not sufficient condition to demonstrate the presence of light−matter coherent coupling. On the contrary an anticrossing behavior of the energy peaks is the signature of such a strong coupling regime.[40] This is clearly shown in Figure 2b for a microcavity at a coupling value of 14%.

A complete optical characterization has been performed for each microcavity, which for easiness of reading it is summarized by plotting only the normalized lower and upper polariton energy peaks in Figure 2c. Solid dots are the experimental data for the diluted microcavities, while the open dots are those for the heterostructure microcavities. In both cases experimental data have been plotted at zero exciton-cavity detuning.

We have seen so far that our system is strongly coupled. However, the transition from the strong coupling to the ultrastrong regime, by increasing the number of absorbing dipoles, is not sharp but rather smooth. The best way to define the USC regime is to back the data with a theory that takes into account the antirotating terms. The polariton energies can be described analytically by the eigenvalues of the Hopfield Hamiltonian of the interacting system,[19,41,42] which are provided by the solutions of the equation

$$(E_c^2 - E^2)(\tilde{E}_0^2 - E^2) = g^2 E_0^2 E_c^2 \quad (2)$$

where E_0 is the exciton energy, $E_c^2 = E_c^2(0) + E^2 \sin\theta^2/\epsilon_h$ describes the energy dispersion of the cavity mode, ϵ_h is the dielectric constant at high frequencies (just beyond the material absorption band), and $\tilde{E}_0^2 = E_0^2 + g^2 E_0^2/f_w$, where f_w describes the overlap between the cavity mode and the resonant layer (for an active layer fully occupying the cavity volume $f_w = 1$). The solutions of eq 2 give the lower (E_-) and the upper (E_+) polariton dispersion energies of the corresponding eigenstates of the Hopfield Hamiltonian. In the SC case the contributions of the antiresonant terms are negligible and the polariton eigenvalues, at resonance conditions (namely, $E_0 = E_c$), can be approximated by a linear dependence on g:

$$E_\mp \cong E_0\left(1 \mp \frac{g}{2}\right) \quad (3)$$

Figure 2c shows the upper and lower polariton energies normalized to the exciton energy for the above samples as a function of the coupling factor. As we can see in Figure 2c, the linear regime is followed only up to a coupling ratio of about 25%. Above this coupling value the deviation from the linear plot is clear, which is an evident indication of the USC regime.[13] In this case the exact solution of the Hopfield Hamiltonian must be used, which is given, at zero detuning, by the following equation:

$$E_\mp = E_0\left(\sqrt{1 + \frac{g^2}{4}} \mp \frac{g}{2}\right) \quad (4)$$

This is confirmed by the excellent match of the polariton energies (filled and open dots) all along the solid lines of Figure 2c.

Another interesting feature of the USC regime is the opening of a forbidden polariton energy gap, where no eigenstate polariton solutions can be found.[19,20] In Figure 2d we plotted the polariton energy maxima as a function of the cavity thickness at a coupling of 54%. The continuous lines are the best fit of the data with the solutions of eq 2. The straight lines (asymptotes), delimiting the polaritonic gap, have been obtained taking the low- and high-frequency limits of the solutions of eq 2. The asymptotes gave a forbidden polaritonic energy gap ΔE_{gap} of 267 meV. A similar feature has also been observed for inorganic microcavities working in the USC regime but in the THz spectral region.[19,20,38] However, given the very small energy transition of those systems, our energy gap of 267 meV is for instance more than 2 orders of magnitude larger than in ref 20 and could be exploited for the realization of metamaterials working in the mid-infrared region, given that in the forbidden energies of the gap the system behaves as a material with negative refractive index.[43]

We now demonstrate that these features of the USC regime are clearly visible also when the microcavity is excited by electrical injection.[44,24] The device structure used to demonstrate the electroluminescence (EL) in the USC regime is illustrated in Figure 3a. We realized monolithic microcavity-OLEDs (MCOLEDs) using high-vacuum thermally evaporable organic materials, which enable a fine control of the thickness layers. The devices, realized on indium tin oxide-coated glass,

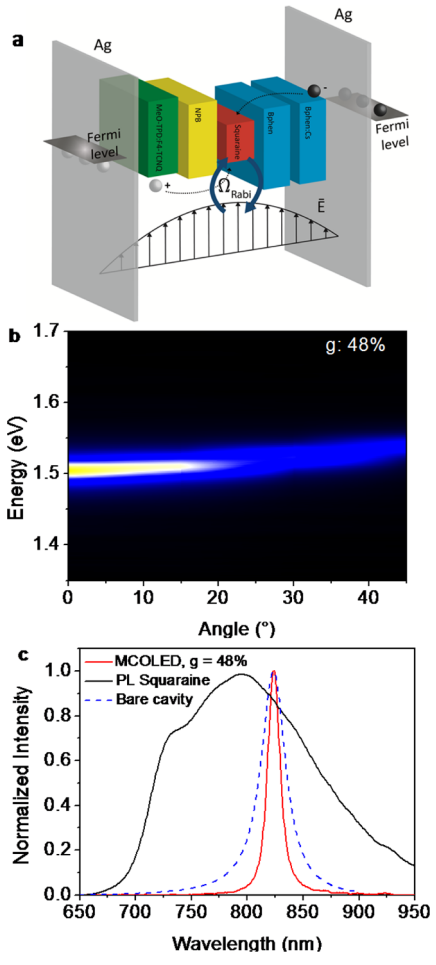

Figure 3. Schematic, optical, and EL characterizations of MCOLEDs in USC. (a) Scheme of an MCOLED with the energy-level diagram of the organic layers illustrating the two-step mechanism of charge injection and exciton formation within the squaraine dye. (b) Contour plots of the angle-resolved EL spectrum of the MCOLED at 48% coupling and at zero detuning. (c) Normalized EL spectrum of an MCOLED at g = 48% (red line), PL spectrum of a neat film of squaraine with a thickness of 60 nm (black line), and transmission spectrum of a bare (empty) cavity (dashed line).

dx.doi.org/10.1021/ph500266d | ACS Photonics 2014, 1, 1042−1048

have the following structure: Ag/p/EBL/EML/HBL/n/Ag (see Figure 3a). Here p and n layers stand for the hole and the electron doped transporting layers, while EBL and HBL are the electron- and hole-blocking layers, respectively (see Methods for further information). These layers do not play any active role in the light−matter coupling, but they act as optical spacers. The emissive layer (EML) is then placed exactly at the antinode position of the electromagnetic field, where the field intensity reaches its maximum (Figure 3a). Furthermore, the energetic levels of the active layer allow an efficient confinement of excitons in a quantum-well-like structure, maximizing the light−matter coupling. The polariton states are electrically pumped using the p−i−n technology, which allows a good injection of carriers independently from the electrodes used, thus making possible the use of silver mirrors as both anode and cathode.[45] Figure S3 shows the transmission spectra of an MCOLED working at a coupling value of 48%. This device, which consists of a squaraine active layer of 60 nm, was the best trade-off between the optical coupling parameters and the electrical constraints. Figure 3b reports the measured EL spectra of the LP branch against the output angle, showing that the EL dispersion follows the LP transmittance (Figure S3). The lower polariton EL energies are spanned in a range from 1.51 eV at 0° to 1.54 eV at 45°, which corresponds to a total blue-shift of only 30 meV.

Figure 3c shows the photoluminescence (PL) spectrum of a neat squaraine film having a full width at half maximum (FWHM) of 440 meV. Despite the very large PL linewidth, we observe an ultranarrow polariton EL (Figure 3c). The polariton FWHM is only 28 meV, 12-fold narrower than the PL emission and even narrower than the bare cavity linewidth (50 meV). In order to study the FWHM as a function of the exciton-cavity detuning, we consider several MCOLEDs with different cavity thicknesses but with the same coupling factor, g = 30%. This can be done keeping constant the squaraine layer thickness (20 nm), while varying the total thickness of the cavity in a range spanning from 80 nm up to 200 nm. The EL linewidth of the LP branches at k = 0, shown in Figure 4a, reached the minimum value of 32 meV as the resonant condition (zero detuning) is approached. We ascribe this effect to the collective coupling of the inhomogeneous excitons with the cavity, which results in a system that behaves like a single exciton with a very strong oscillator strength coupled coherently with the cavity. This is confirmed by the Lorentzian shape of the lower polariton emission. As reported by Houdrè et al.,[34] for microcavities coupling with an inhomogeneously broadened system, when the Rabi splitting is larger than the inhomogeneous linewidth, the polariton linewidths are given by half the sum between the cavity linewidth γ_c and the homogeneous exciton linewidth γ_{hom}. It is also worth noting that moving from the resonant condition in the direction of either negative or positive detunings, the effective coupling strength decreases and the polariton linewidth broadens (Figure 4a). This analysis is further confirmed by Figure 4b, where the linewidth of the EL emission from the LP is plotted against the coupling strength together with the bare cavity FWHM. Both LP and bare cavity linewidths decrease with increasing coupling just because the reflectivity of silver mirrors at low energies results in a better cavity quality factor, despite that the polariton linewidth decreases faster than that of the cavity. This can be ascribed to the better homogeneous line selection caused by increasing the strength of the coupling. When g is changed from 14% to 60%, the polariton EL linewidth decreases from 45 meV down to 25 meV, while the cavity FWHM changes from 70 meV to 50 meV. The narrowing in the optical spectra of the polariton modes earlier attributed to the motional narrowing effect[46] finds its explanation in a semiclassical theory,[47,48] which assumes an energy distribution of the exciton states, which are related to the disordered nature of our system (amorphous material). In this semiclassical model the narrower polariton line shape is obtained by directly taking into account in the dielectric susceptibility of the system the inhomogeneous frequency distribution of excitons.[48,49] These results open the way to the development of monochromatic microcavity sources with no angular dependence and with very sharp emission below the limit imposed by the cavity itself.

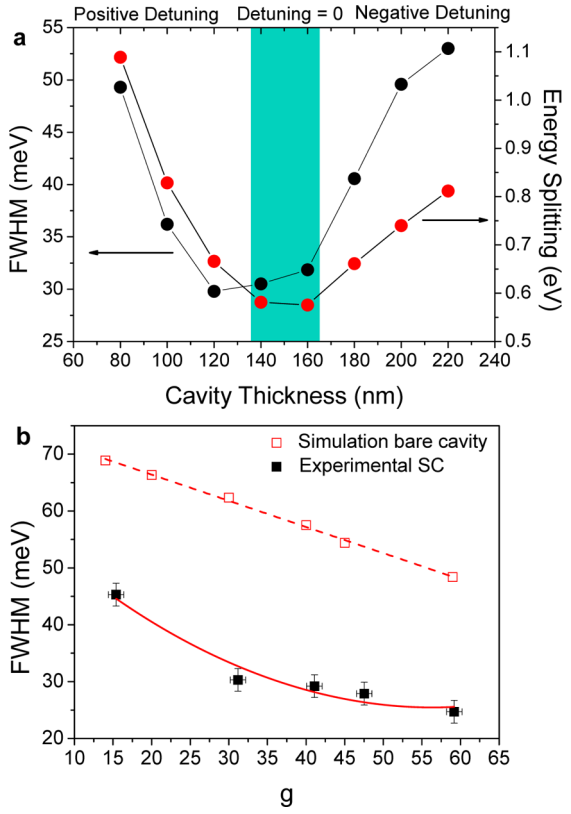

Figure 4. Effect of exciton broadening on the polariton linewidths and coupling. (a) Full width at half maximum (FWHM) of LP electroluminescence (black dots) and energy splitting (red dots) against the cavity thickness for an MCOLED at g = 30%. The minimum in the linewidth is reached at zero detuning (minimum of energy splitting), corresponding to a cavity thickness between 140 and 160 nm (blue range). (b) FWHM of LP electroluminescence (filled dots) and of bare cavities (empty dots) against the coupling strength.

CONCLUSIONS

In conclusion, we have observed ultrastrong light−matter coupling at room temperature in planar microcavities consisting of a thin film of squaraine dye embedded between two silver mirrors and in a multilayer monolithic microcavity-OLED having the same active layer. Despite the broad inhomogeneous absorption spectrum of the active layer, our results are an unambiguous proof of the USC regime with coherent energy exchange between photon and exciton, and it opens the way to the use of a wider range of materials so far neglected for their optical properties. Furthermore, thanks to the USC regime, we were able to achieve a polariton emission that is more than an

dx.doi.org/10.1021/ph500266d | ACS Photonics 2014, 1, 1042−1048

order of magnitude narrower than the bare film luminescence and half the linewidth emission of a photonic microcavity tuned at the same emissive wavelength. This feature might be very useful for several optical applications that require a high color purity without having to deal with more demanding architectures, such as the use of dielectric mirrors (DBR) to improve the cavity finesse. Moreover due to the USC properties of the MCOLEDs, it is possible to have angular-independent electroluminescence with nearly monochromatic emission.

METHODS

Sample Preparation. Samples were fabricated on commercially available glass substrates. Substrates were sonicated in acetone and isopropyl alcohol before drying with nitrogen. Both neat and blend organic layers were grown by thermal evaporation in a high-vacuum chamber (1×10^{-6} mbar) at a deposition rate of 0.1 nm/s. Metal mirrors were grown by thermal evaporation in a high-vacuum chamber (1×10^{-6} mbar) at a deposition rate of 0.05 nm/s.

For the microcavity-OLED fabrication, we used the following layer structure: Ag (40 nm)/p (X nm)/EBL (10 nm)/EML (Y nm)/HBL (10 nm)/n (X nm)/Ag (40 nm), with X values varying as a function the total cavity thickness and thus the detuning and Y values varying as a function of the MCOLED coupling ratio. The p-doped layer has been realized by co-deposition of the dopant molecules of 2,3,5,6-tetrafluoro-7,7,8,8-tetracyanoquinodimethane (F4TCNQ) into a matrix of *N*,*N*,*N*′,*N*′-tetrakis (4-methoxyphenyl)benzidine (MeOTPD); the n-doped layer consists of 4,7-diphenyl-1,10-phenanthroline (Bphen) doped with Cs. In our case the EBL consists of NPB, meanwhile the HBL consists of Bphen. The EML is the emitting layer and consists of a neat film of squaraine dye. Silver has been used as both anode and cathode despite its poor hole injection properties. This problem has been overcome by using a p−i−n technology, where the p and n transport layers have been lightly doped to reduce the ohmic losses to a negligible level and allow for a tunneling injection of the carriers from the metal layers.

Transmittance Measurements. Cavity transmission spectra were recorded using a J.A. Wollam M-2000XI ellipsometer. Measurements were performed irradiating the sample with a white light and recording the signal at different angles of light incidence.

Photophysical Characterization. For absorption measurements films on glass, without the bottom and top mirrors, were prepared under the same experimental conditions as the same layer within the microcavity. Measurements were carried out by a Varian Cary Eclipse spectrophotometer.

Electrical Characterization. The EL spectrum and power emission have been recorded through an angle rotating stage coupled to a vis−NIR optical fiber.

ASSOCIATED CONTENT

Supporting Information

Detailed description of the optical microcavity preparation and structure. Materials chemical formula. Microcavity-OLED optical transmittance dispersion. Squaraine solution absorption spectrum. This material is available free of charge via the Internet at http://pubs.acs.org.

AUTHOR INFORMATION

Corresponding Author

*E-mail: marco.mazzeo@unisalento.it.

Notes

The authors declare no competing financial interest.

ACKNOWLEDGMENTS

We thank S. Carallo and A. Melcarne for technical support. We are grateful to S. De Liberato and S. Kena-Cohen for fruitful and inspiring discussions. This work was supported by EFOR-Energia da Fonti Rinnovabili (Iniziativa CNR per il Mezzogiorno L. 191/2009 art. 2 comma 5544), MAAT (MIUR-PON02_00563_3316357-CUP B31C12001230005), Rete di Laboratori della Regione Puglia PHOEBUS, progetto 5 per mille per la ricerca "Realizzazione di dispositivi organici in regime di strong coupling" (CUP F81J2000660001), and MIUR project Beyond Nano and the ERC project POLA-FLOW (grant 308136).

REFERENCES

(1) Kasprzak, J.; Richard, M.; Kundermann, S.; Baas, A.; Jeambrun, P.; Keeling, J. M. J.; Marchetti, F. M.; Szymanska, M. H.; Andre, R.; Staehli, J. L.; Savona, V.; Littlewood, P. B.; Deveaud, B.; Dang, L. S. Bose−Einstein condensation of exciton polaritons. *Nature* **2006**, *443*, 409−414.

(2) Balili, R.; Hartwell, V.; Snoke, D.; Pfeiffer, L.; West, K. Bose−Einstein condensation of microcavity polaritons in a trap. *Science* **2007**, *316*, 1007−1010.

(3) Kéna-Cohen, S.; Forrest, S. R. Room-temperature polariton lasing in an organic single-crystal microcavity. *Nat. Photonics* **2010**, *4*, 371−375.

(4) Amo, A.; Sanvitto, D.; Laussy, F. P.; Ballarini, D.; Valle, E. d.; Martin, M. D.; Lemaitre, A.; Bloch, J.; Krizhanovskii, D. N.; Skolnick, M. S.; Tejedor, C.; Vina, L. Collective fluid dynamics of a polariton condensate in a semiconductor microcavity. *Nature* **2009**, *457*, 291−295.

(5) Amo, A.; Lefrere, J.; Pigeon, S.; Adrados, C.; Ciuti, C.; Carusotto, I.; Houdre, R.; Giacobino, E.; Bramati, A. Superfluidity of polaritons in semiconductor microcavities. *Nat. Phys.* **2009**, *5*, 805−810.

(6) Sanvitto, D.; Marchetti, F. M.; Szymanska, M. H.; Tosi, G.; Baudisch, M.; Laussy, F. P.; Krizhanovskii, D. N.; Skolnick, M. S.; Marrucci, L.; Lemaitre, A.; Bloch, J.; Tejedor, C.; Vina, L. Persistent currents and quantized vortices in a polariton superfluid. *Nat. Phys.* **2010**, *6*, 527−533.

(7) Sanvitto, D.; Pigeon, S.; Amo, A.; Ballarini, D.; De Giorgi, M.; Carusotto, I.; Hivet, R.; Pisanello, F.; Sala, V. G.; Guimaraes, P. S. S.; Houdre, R.; Giacobino, E.; Ciuti, C.; Bramati, A.; Gigli, G. All-optical control of the quantum flow of a polariton condensate. *Nat. Photonics* **2011**, *5*, 610−614.

(8) Ballarini, D.; De Giorgi, M.; Cancellieri, E.; Houdré, R.; Giacobino, E.; Cingolani, R.; Bramati, A.; Gigli, G.; Sanvitto, D. All-optical polariton transistor. *Nat. Commun.* **2013**, *4*, 1778−1778.

(9) Monroe, C. Quantum information processing with atoms and photons. *Nature* **2002**, *416*, 238−246.

(10) Scalari, G.; Maissen, C.; Turčinková, D.; Hagenmüller, D.; De Liberato, S.; Ciuti, C.; Reichl, C.; Schuh, D.; Wegscheider, W.; Beck, M.; Faist, J. Ultrastrong coupling of the cyclotron transition of a 2D electron gas to a THz metamaterial. *Science* **2012**, *335*, 1323−1326.

(11) Forn-Díaz, P.; Lisenfeld, J.; Marcos, D.; García-Ripoll, J. J.; Solano, E.; Harmans, C. J. P. M.; Mooij, J. E. Observation of the Bloch-Siegert shift in a qubit-oscillator system in the ultrastrong coupling regime. *Phys. Rev. Lett.* **2010**, *105*, 237001−237001.

(12) Geiser, M.; Castellano, F.; Scalari, G.; Beck, M.; Nevou, L.; Faist, J. Ultrastrong coupling regime and plasmon polaritons in parabolic semiconductor quantum wells. *Phys. Rev. Lett.* **2012**, *108*, 106402−106402.

(13) Ciuti, C.; Bastard, G.; Carusotto, I. Quantum vacuum properties of the intersubband cavity polariton field. *Phys. Rev. B* **2005**, *72*, 115303−115303.
(14) Gunter, G.; Anappara, A. A.; Hees, J.; Sell, A.; Biasiol, G.; Sorba, L.; De Liberato, S.; Ciuti, C.; Tredicucci, A.; Leitenstorfer, A.; Huber, R. Sub-cycle switch-on of ultrastrong light-matter interaction. *Nature* **2009**, *458*, 178−181.
(15) Anappara, A. A.; De Liberato, S.; Tredicucci, A.; Ciuti, C.; Biasiol, G.; Sorba, L.; Beltram, F. Signatures of the ultrastrong light-matter coupling regime. *Phys. Rev. B* **2009**, *79*, 201303−201303.
(16) Stassi, R.; Ridolfo, A.; Di Stefano, O.; Hartmann, M. J.; Savasta, S. Spontaneous Conversion from Virtual to Real Photons in the Ultrastrong-Coupling Regime. *Phys. Rev. Lett.* **2013**, *110*, 243601−243601.
(17) Ridolfo, A.; Leib, M.; Savasta, S.; Hartmann, M. J. Photon blockade in the ultrastrong coupling regime. *Phys. Rev. Lett.* **2012**, *109*, 193602−193602.
(18) Ridolfo, A.; Savasta, S.; Hartmann, M. J. Nonclassical radiation from thermal cavities in the ultrastrong coupling regime. *Phys. Rev. Lett.* **2013**, *110*, 163601−163601.
(19) Todorov, Y.; Andrews, A. M.; Colombelli, R.; De Liberato, S.; Ciuti, C.; Klang, P.; Strasser, G.; Sirtori, C. Ultrastrong light-matter coupling regime with polariton dots. *Phys. Rev. Lett.* **2010**, *105*, 196402−196402.
(20) Jouy, P.; Vasanelli, A.; Todorov, Y.; Delteil, A.; Biasiol, G.; Sorba, L.; Sirtori, C. Transition from strong to ultrastrong coupling regime in mid-infrared metal-dielectric-metal cavities. *Appl. Phys. Lett.* **2011**, *98*, 231114−231114.
(21) Lidzey, D. G.; Bradley, D. D. C.; Skolnick, M. S.; Virgili, T.; Walker, S.; Whittaker, D. M. Strong exciton-photon coupling in an organic semiconductor microcavity. *Nature* **1998**, *395*, 53−55.
(22) Schwartz, T.; Hutchison, J. A.; Genet, C.; Ebbesen, T. W. Reversible switching of ultrastrong light-molecule coupling. *Phys. Rev. Lett.* **2011**, *106*, 196405−196405.
(23) Kéna-Cohen, S.; Maier, S. A.; Bradley, D. D. C. Ultrastrongly coupled exciton−polaritons in metal-clad organic semiconductor microcavities. *Adv. Opt. Mater.* **2013**, *1*, 827−833.
(24) Mazzeo, M.; Genco, A.; Gambino, S.; Ballarini, D.; Mangione, F.; Di Stefano, O.; Patanè, S.; Savasta, S.; Sanvitto, D.; Gigli, G. Ultrastrong light-matter coupling in electrically doped microcavity OLEDs. *Appl. Phys. Lett.* **2014**, *104*, 233303−233303.
(25) McKeever, J.; Boca, A.; Boozer, A. D.; Buck, J. R.; Kimble, H. J. Experimental realization of a one-atom laser in the regime of strong coupling. *Nature* **2003**, *425*, 268−271.
(26) Deing, K. C.; Mayerhoffer, U.; Wurthner, F.; Meerholz, K. Aggregation-dependent photovoltaic properties of squaraine/PC61BM bulk heterojunctions. *Phys. Chem. Chem. Phys.* **2012**, *14*, 8328−8334.
(27) Wang, S.; Mayo, E. I.; Perez, M. D.; Griffe, L.; Wei, G.; Djurovich, P. I.; Forrest, S. R.; Thompson, M. E. High efficiency organic photovoltaic cells based on a vapor deposited squaraine donor. *Appl. Phys. Lett.* **2009**, *94*, 233304−233304.
(28) Chen, G.; Yokoyama, D.; Sasabe, H.; Hong, Z.; Yang, Y.; Kido, J. Optical and electrical properties of a squaraine dye in photovoltaic cells. *Appl. Phys. Lett.* **2012**, *101*, 083904−083904.
(29) Tischler, J. R.; Bradley, M. S.; Bulović, V.; Song, J. H.; Nurmikko, A. Strong coupling in a microcavity LED. *Phys. Rev. Lett.* **2005**, *95*, 036401−036401.
(30) Ashwell, G. J.; Jefferies, G.; Hamilton, D. G.; Lynch, D. E.; Roberts, M. P. S.; Bahra, G. S.; Brown, C. R. Strong second-harmonic generation from centrosymmetric dyes. *Nature* **1995**, *375*, 385−388.
(31) Ballarini, D.; De Giorgi, M.; Gambino, S.; Lerario, G.; Mazzeo, M.; Genco, A.; Accorsi, G.; Giansante, C.; Colella, S.; D'Agostino, S.; Cazzato, P.; Sanvitto, D.; Gigli, G. Polariton-Induced Enhanced Emission from an Organic Dye under the Strong Coupling Regime. *Adv. Opt. Mater.* **2014**, DOI: 10.1002/adom.201400226.
(32) Yeh, A. P. *Optical Waves in Layered Media*; J. Wiley & Sons: Hoboken, NJ, 2005.
(33) Nitsche, R.; Fritz, T. Determination of model-free Kramers-Kronig consistent optical constants of thin absorbing films from just one spectral measurement: application to organic semiconductors. *Phys. Rev. B* **2004**, *70*, 195432−195432.
(34) Houdré, R.; Stanley, R. P.; Ilegems, M. Vacuum-field Rabi splitting in the presence of inhomogeneous broadening: resolution of a homogeneous linewidth in an inhomogeneously broadened system. *Phys. Rev. A* **1996**, *53*, 2711−2715.
(35) Cooke, D. W.; Bennett, B. L.; McClellan, K. J.; Roper, J. M.; Whittaker, M. T.; Portis, A. M. Electron-lattice coupling parameters and oscillator strengths of cerium-doped lutetium oxyorthosilicate. *Phys. Rev. B* **2000**, *61*, 11973−11978.
(36) We notice that, in contrast to Figure 1a, the upper polariton line for the sample with the neat film is partially affected by inhomogeneous broadening. This is due to the high amount of broadening in the high-energy part of the polariton absorbance as compared to the rather small Rabi splitting.
(37) Houdré, R. Early stages of continuous wave experiments on cavity-polaritons. *Phys. Status Solidi B* **2005**, *242*, 2167−2196.
(38) Delteil, A.; Vasanelli, A.; Todorov, Y.; Feuillet Palma, C.; Renaudat St-Jean, M.; Beaudoin, G.; Sagnes, I.; Sirtori, C. Charge-induced coherence between intersubband plasmons in a quantum structure. *Phys. Rev. Lett.* **2012**, *109*, 246808−246808.
(39) Askenazi, B.; Vasanelli, A.; Delteil, A.; Todorov, Y.; Andreani, L.; Beaudoin, G.; Sagnes, I.; Sirtori, C. Ultra-strong light-matter coupling for designer Reststrahlen band. *New J. Phys.* **2014**, *16*, 043029−043029.
(40) Kavokin, A. V.; Baumberger, J. J.; Malpuech, G.; Laussy, F. P. *Microcavities*; Oxford University Press, 2007.
(41) Quattropani, A.; Andreani, L. C.; Bassani, F. Quantum theory of polaritons with spatial dispersion: exact solutions. *Il Nuovo Cimento D* **1986**, *7*, 55−69.
(42) Hopfield, J. J. Theory of the contribution of excitons to the complex dielectric constant of crystals. *Phys. Rev.* **1958**, *112*, 1555−1567.
(43) Jun, Y. C.; Reno, J.; Ribaudo, T.; Shaner, E.; Greffet, J.-J.; Vassant, S.; Marquier, F.; Sinclair, M.; Brener, I. Epsilon-near-zero strong coupling in metamaterial-semiconductor hybrid structures. *Nano Lett.* **2013**, *13*, 5391−5396.
(44) Gubbin, C. R.; Maier, S. A.; Kéna-Cohen, S. Low-voltage polariton electroluminescence from an ultrastrongly coupled organic light-emitting diode. *Appl. Phys. Lett.* **2014**, *104*, 233302−233302.
(45) Mazzeo, M.; Mariano, F.; Genco, A.; Carallo, S.; Gigli, G. High efficiency ITO-free flexible white organic light-emitting diodes based on multi-cavity technology. *Org. Electron.* **2013**, *14*, 2840−2846.
(46) Whittaker, D. M.; Kinsler, P.; Fisher, T. A.; Skolnick, M. S.; Armitage, A.; Afshar, A. M.; Sturge, M. D.; Roberts, J. S. Motional narrowing in semiconductor microcavities. *Phys. Rev. Lett.* **1996**, *77*, 4792−4795.
(47) Kavokin, A. V. Motional narrowing of inhomogeneously broadened excitons in a semiconductor microcavity: semiclassical treatment. *Phys. Rev. B* **1998**, *57*, 3757−3760.
(48) Kavokin, A. V.; Baumberg, J. J. Exciton-light coupling in quantum wells: from motional narrowing to superradiance. *Phys. Rev. B* **1998**, *57*, R12697−R12700.
(49) Kavokin, A. V.; Malpuech, G.; Panzarini, G. Inhomogeneous Broadening of Excitons in Thin Films of GaN: effect on the time-resolved transmission spectra. *Phys. Status Solidi B* **1999**, *216*, 31−34.